

# High resolution spectroscopy of giant HII regions around young massive clusters<sup>★</sup>

L. Vanzi<sup>1</sup>, A. Scatarzi<sup>2</sup>, R. Maiolino<sup>2</sup>, and M. Sterzik<sup>1</sup>

<sup>1</sup> European Southern Observatory, Alonso de Cordova 3107, Vitacura, Santiago, Chile  
e-mail: [lvanzi;msterzick]@eso.org

<sup>2</sup> Osservatorio Astrofisico di Arcetri, Largo E. Fermi 5, 50125 Firenze, Italy  
e-mail: [scatarzi;maiolino]@arcetri.astro.it

Received 25 July 2005 / Accepted 12 June 2006

## ABSTRACT

We present new high-resolution optical spectroscopy of giant HII regions around three young massive clusters located in the blue dwarf galaxies NGC 5253 and He 2-10. We used the observations to derive the mass of the clusters under the hypothesis of virialization. The virial masses exceed the optical ones. In one case, however, the virial mass is consistent with that derived from the IR luminosity, pointing to the presence of a hidden stellar population. The dynamics inferred from the emission lines indicates that the clusters may indeed be virialized or close to virialization. We detect an indication of mass segregation in two clusters. At least in one case, we find that such mass segregation must have a “primordial” nature, rather than dynamical, i.e. associated with the formation mechanism of the cluster. We could resolve two of the clusters with the spectro-astrometric technique detecting in both cases evidence of structures on the pc scale.

**Key words.** galaxies: dwarf – galaxies: individual: NGC 5253 – galaxies: individual: He 2-10 – galaxies: star clusters

## 1. Introduction

Young massive clusters (YMC) have been detected in a large number of galaxies characterized by high star-formation rates: interacting (Whitmore et al. 1999); giants (Larsen & Richtler 1999; Larsen 2000); dwarfs (McCraday et al. 2005; Vanzi & Sauvage 2006) and AGNs (Galliano et al. 2005). Some of these galaxies host few YMCs, others up to a few hundred. It is becoming evident that YMCs are very important in the star formation process occurring in galaxies and possibly in the formation of galaxies themselves. They account for a large fraction of the overall star formation in some cases, and their winds and ionizing output can be relevant to the properties and evolution of the hosting system. The luminosity and mass of YMCs are typically distributed according to a power law (Whitmore et al. 1999; Johnson et al. 2000; Larsen 2002; Cresci et al. 2005; Vanzi & Sauvage 2006), and evidence has been collected to show that this power law could evolve toward the distribution observed for globular clusters, with the less massive clusters being evaporated, while the most massive and gravitationally bound ones survive over a Hubble time (Fall & Rees 1977; Fall & Zhang 2001). Typical masses of YMCs are in the range  $10^4$ – $10^6 M_{\odot}$ . It is also becoming evident that in their early phases, YMCs are deeply embedded in dust and molecular clouds. The embedded phase is estimated to last only a few Myrs.

We obtained high dispersion spectroscopy in the visible band of three classical YMCs with the purpose of characterizing their properties and those of the surrounding medium. Two of the observed clusters are located in NGC 5253, a well-known blue dwarf galaxy characterized by a recent episode of star formation, a large number of clusters (van den Bergh 1980),

and sub-solar abundances (Kobulnicky et al. 1999). In this paper we have assumed a distance to NGC 5253 of 3.3 Mpc (Gibson et al. 2000). The clusters observed in NGC 5253 are numbers 1 and 5 following the nomenclature of Calzetti et al. (1997). Their ages are 8–12 Myr and 2.5–4.4 Myr, respectively, according to the HST observations of Calzetti et al. (1997). The estimated stellar masses are  $<4 \times 10^5 M_{\odot}$  and about  $2$ – $3 \times 10^5 M_{\odot}$ , respectively, again according to the estimates of Calzetti et al. (1997). Vanzi & Sauvage (2004) instead derive a total mass of  $0.82$ – $2.1 \times 10^6 M_{\odot}$  and an age younger than 2 Myr for cluster 5 from a careful modeling of the IR emission of the cluster. The discrepancy by almost one order of magnitude between the optical and IR estimate of the mass is not surprising since it has been found that NGC 5253-5 is embedded in dust and extinguished by about 8 magnitudes in the optical, so that a large fraction of its stellar content could easily escape optical observations. The third cluster is located in He 2–10, which is also a blue dwarf galaxy at a distance of 9 Mpc (Johansson 1987). This cluster is identified as “A” by Johnson et al. (2000) who derive a mass of  $1.6$ – $2.6 \times 10^6 M_{\odot}$ . The age of the cluster is estimated to be about 3–6 Myr based on the presence of WR stars.

This paper is organized as follows, we briefly describe the observations in Sect. 2, and in Sect. 3 we present the analysis of the data including line profiles, reddening, ionization status of the interstellar medium, and spectro-astrometry. In Sect. 4 we summarize our conclusions.

## 2. Observations

The observations were obtained during the nights of March 13 and March 15, 2003, at the ESO - VLT with the red arm of the cross-dispersed echelle spectrometer UVES. The spectral range covered is 4800–5680 Å and 5840–6715 Å with a gap

<sup>★</sup> Based on observations obtained at the ESO - VLT under program 270.B-5037.

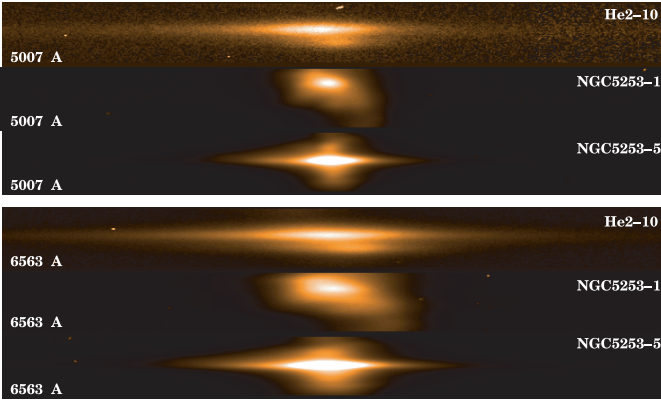


**Fig. 1.** Two dimensional spectra centered on [OIII]5007 and  $H\alpha$  of the HII regions observed. The spatial dimension is  $12''$  wide.

produced by the fact that the spectrum is imaged on two CCDs separated by 1 mm. We used a slit of  $0.5'' \times 12''$ , oriented as the parallactic angle, obtaining a spectral resolution of about 80 000. The spatial scale along the slit is  $0.182''$  per pixel. The integration time was 60 min divided in three 20-min exposures for NGC 5253-1 and NGC 5253-5 and 15 min divided in 15 1-min exposures for the cluster in He 2-10. The seeing during the observations was about  $1''$ . The spectra were reduced using the UVES pipeline provided by ESO. The wavelength calibration was obtained using a Th-Ar comparison spectrum. Two dimensional spectra,  $12''$  wide, centered on [OIII]5007 and  $H\alpha$  are shown in Fig. 1. One dimensional spectra were extracted from the 2D spectra with a width of 3 pixels, corresponding to apertures of about  $0.5'' \times 0.5''$ . A spectrum of the star LTT 3218 observed with a slit  $5'' \times 12''$  was used for the calibration in flux, the data reduction was done in MIDAS. The 2D spectrum of the star was smoothed to a resolution of  $50 \text{ \AA}$  and compared to the template of Hamuy et al. (1992) to derive a 2D instrument response curve.

### 3. Analysis

The new observations were used to derive the properties of the giants HII regions and the ionizing clusters.

#### 3.1. Line profiles

In Fig. 2 we show the profiles of  $H\alpha$  for the three clusters, centered on the center of the cluster and extracted with an aperture of 3 pixels so that the final aperture is about  $0.5'' \times 0.5''$ . We used ALICE in MIDAS to fit the line profiles. It was not possible to obtain satisfactory fits with a single Gaussian and, in all cases, at least two Gaussian components were necessary. The parameters of the fits are given in Table 1 for  $H\alpha$ , [OIII] 5007, and [NII] 6583. We estimated the global error on the line fluxes to be on the order of 1%, which includes the statistical error and the error introduced by the calibrations. The error on the velocities can be estimated by examining the values in Table 1 for different spectral lines, and it is typically less than  $2 \text{ km s}^{-1}$ .

In the case of He 2-10 and NGC 5253-5, the two-component fit gives a relatively narrow component superimposed on a significantly broader one (a factor of about 3–4 broader than the narrow component), in agreement with the multiple “narrow” components superimposed on a single broader one found by Melnick et al. (1999) in the HII region surrounding 30-Doradus. The case of NGC 5253-1 is different, because the line profile

observed is affected by the presence of a region located at about  $2''$  to the north and characterized by very strong emission lines that extend toward the cluster and blend with it, see Fig. 1. This region is very close to the cluster NGC 5253-4, though it cannot be identified with it. The small Gaussian component observed in this case is almost certainly the tail of the emission lines from the neighboring region. The fact that, unlike Melnick et al. (1999) we detect, in all cases, a single narrow component can be attributed to the fact that our aperture averages over a much larger physical region due to the greater distance of the targets. The  $\sigma$  of the broad components agree with the observation of Melnick et al. (1999), who attribute this component to a tenuous highly turbulent gas.

The broadening of the emission lines in HII regions is produced by a few fundamental effects, as described by Melnick et al. (1999): mainly thermal broadening, virial broadening, and local dynamical effects as expanding shells, filaments, and outflows. Terlevich & Melnick (1981) and Rozas et al. (1998) report observing an empirical correlation between the total  $H\beta$  or  $H\alpha$  luminosity of giant HII regions and their observed  $\sigma$ . This correlation can be conceptually understood if the  $\sigma$  is mostly determined by gravity. The HII regions must be virialized or almost virialized. In this case, an estimate of the mass can be derived. To compare our observations with this empirical relation, we extracted 1D spectra with an aperture that includes most of the  $H\alpha$  emission along the slit and repeated the double-component fit, the results are given in Table 2. The errors on the quantities related to the lines are the same as in Table 1.

To derive the total  $H\alpha$  luminosity, we calculated a slit-loss correction factor assuming the HII regions to be regular and symmetrical. The correction factor turned out to be about 5 in the case of He 2-10 and NGC 5253-5, which were integrated over an aperture equal to the *FWHM* of the spatial profile, but was almost 20 for NGC 5253-1 where, due to the blending with the neighboring region located to the north, we were forced to truncate the spatial integration in that direction. After correcting for the extinction, we obtained  $3.83$ ,  $8.41$ , and  $12.1 \times 10^{39} \text{ erg/s}$  for the total  $H\alpha$  luminosity of NGC 5253-1, NGC 5253-5 and He 2-10, respectively. The slit-loss correction introduces a major source of uncertainty on the fluxes. To evaluate it, we measured the  $H\alpha$  luminosity of cluster 5 on the HST image of Calzetti et al. (1997). We obtained a value of  $5.3 \times 10^{39} \text{ erg/s}$  after correcting for the extinction. This value is about 35% lower than the slit-loss-corrected luminosity obtained from the spectrum, and it gives an estimate of the approximation introduced. The uncertainty is probably larger for NGC 5253-1 due to the larger correction.

In Fig. 3 we compare our data points with the relation of Terlevich & Melnick (1981), converted to  $H\alpha$  assuming a  $H\alpha/H\beta$  ratio of 2.86, and Rozas et al. (1998). Both the total  $H\alpha$  luminosity and the luminosity of the narrow component of the fit are shown, along with the total  $H\alpha$  luminosity before correction for the slit-loss. As  $\sigma$  we used the value of the narrow component deconvolved for the instrumental broadening ( $2.2 \text{ km s}^{-1}$ ) and for a thermal contribution of  $9.1 \text{ km s}^{-1}$  (typical of the HII regions, Melnick et al. 1999). If the broad component of the emission lines is associated to highly turbulent gas (Melnick et al. 1999), it should not be used for dynamical studies. The error-bar indicates the uncertainty introduced by the slit-loss correction estimated as described in the previous paragraph. Given the uncertainties, our data points are consistent with the empirical relation. Under the assumption that the clusters are virialized, or almost virialized, we can therefore derive their virial masses as  $M = \sigma^2 R / G$  from the parameters of Table 2. As radius of the

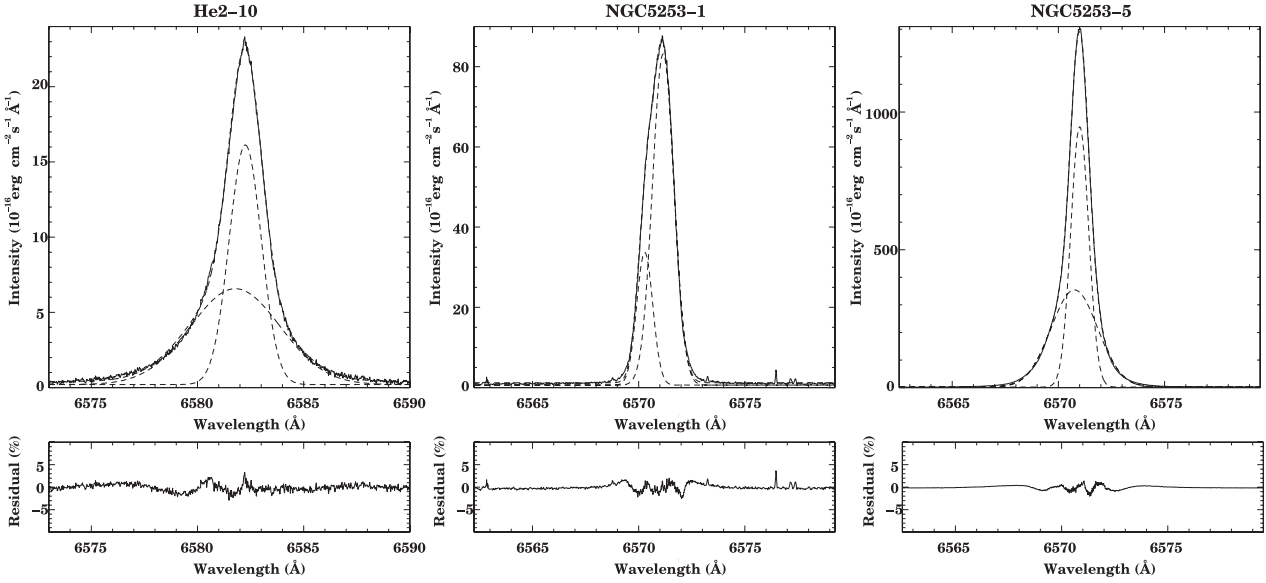


**Fig. 2.** Fit with two Gaussians of the  $H\alpha$  line profiles and associated residuals for the three clusters observed.

**Table 1.** Parameters of the double Gaussian fit executed on the  $H\alpha$ , [OIII] 5007, and [NII] 6583 emission lines. The flux of the components  $F$  is given in  $10^{-16}$  erg/s/cm<sup>2</sup>, position with respect to the nominal center wavelength  $\nu$  and  $\sigma$  are given in km s<sup>-1</sup>.

Name	Line	$F_1$	$\nu_1$	$\sigma_1$	$F_2$	$\nu_2$	$\sigma_2$
5253-1	$H\alpha$	96.9	4.3	22.0	38.3	-34.6	18.5
	[OIII]	90.6	3.3	22.3	23.6	-37.9	15.1
	[NII]	8.0	6.3	19.7	3.0	-33.0	15.5
5253-5	$H\alpha$	997.1	0.6	19.2	968.8	-10.9	49.9
	[OIII]	1496.8	0.7	16.2	1635.5	-8.7	48.6
	[NII]	43.5	2.3	14.2	93.1	-8.6	38.1
He 2-10	$H\alpha$	30.2	1.43	34.2	33.7	-19.0	93.5
	[OIII]	8.4	-1.03	33.9	8.7	-25.9	86.8
	[NII]	9.3	0.9	30.9	9.7	-17.7	87.4

**Table 2.** Parameters of the double Gaussian fit executed on  $H\alpha$  over the bulk of the HII regions. The flux of each component  $F$  is given in  $10^{-15}$  erg/s/cm<sup>2</sup>. The position with respect to the nominal center wavelength  $\nu$  and the  $\sigma$  in km s<sup>-1</sup>. The dimension along the slit, on which the lines were integrated,  $d$  is in ″, this is basically the  $FWHM$  of the spatial profile. The virial masses  $M_{\text{vir}}$  are in units of  $10^6 M_{\odot}$ .

Name	$F_1$	$\nu_1$	$\sigma_1$	$F_2$	$\nu_2$	$\sigma_2$	$d$	$M/\eta$
5253-1	44.9	8.7	23.1	16.2	-27.4	18.5	4.2	1.73
5253-5	248.0	2.0	19.0	254.3	-9.4	49.0	1.6	0.81
He2-10	11.9	1.1	33.8	13.1	-19.5	93.5	2.5	13.3

HII region, we used half  $FWHM$  of the spatial profile along the slit. The values obtained in this way must be multiplied by a factor  $\eta$  that takes into account the relation between  $\sigma$  and the line of sight velocity dispersion and between the gravitational radius and the half light radius  $r_{\text{hl}}$ . A typical value is  $\eta \approx 10$  (e.g. Fleck et al. 2006). For a Gaussian profile, though,  $r_{\text{hl}} \approx FWHM/2$ . In the last column of Table 2 we list  $M/\eta$ .

For NGC 5253-5, Vanzì & Sauvage (2004) derive an upper mass of  $2.1 \times 10^6 M_{\odot}$ , from the integrated IR luminosity. Calzetti et al. (1997) give a mass of  $2-3 \times 10^5 M_{\odot}$ , based on optical observations. There are no IR estimates of the mass of the other two clusters; however, for the most luminous ultra dense HII region of He 2-10, Vacca et al. (2002) derive a mass of about  $10^7 M_{\odot}$

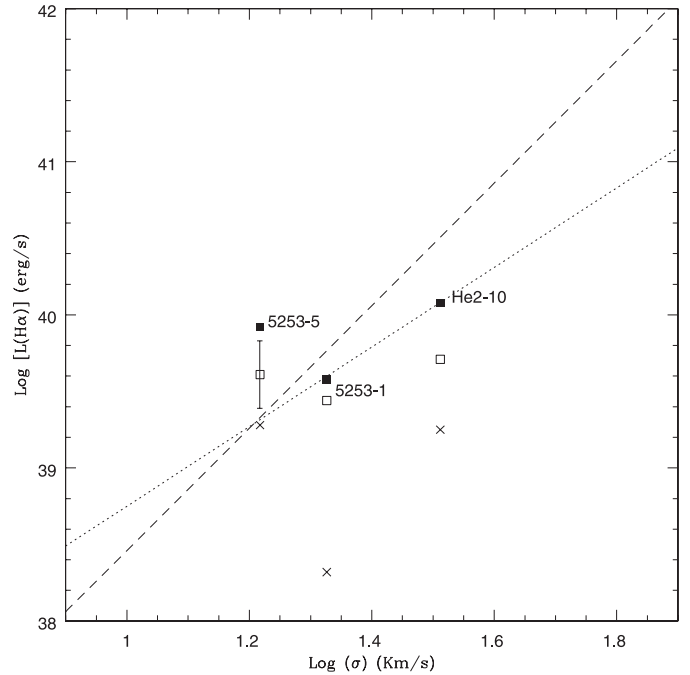


**Fig. 3.** Comparison of the  $H\alpha$  luminosity and  $\sigma$  with the  $L$ - $\sigma$  relationships obtained by Terlevich & Melnick (1981, dashed line) and Rozas et al. (1988, dotted line). Luminosities of the narrow component (open square) and total luminosities (solid squares) are shown, both corrected for slit loss and extinction. The crosses indicate the  $H\alpha$  total luminosities before slit loss correction to give an impression of the effect.

from mid-IR observations. Johnson et al. (2000) instead obtain a mass of  $1.2-2.6 \times 10^6 M_{\odot}$  for region A. Cabanac et al. (2005), however, show that this region can only partially be associated to the optical cluster observed by us. The mass of NGC 5253-5, estimated through the optical luminosity (corrected for extinction by means of the Balmer decrement), falls short by almost one order of magnitude when compared to the IR mass. This discrepancy is most likely due to the fact that a large fraction of the stars in the cluster are obscured. Observations of YMCs in the IR showed in fact that in their early phases they can be

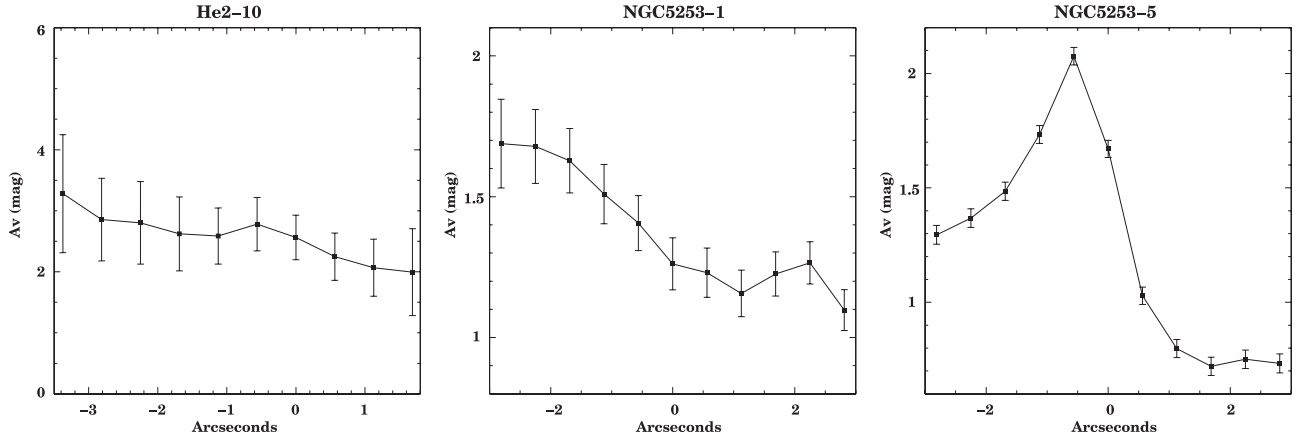


**Fig. 4.** Extinction as function of space along the slit from south (negative) to north (positive) with 0 indicating the position of the cluster.

characterized by very high extinction, largely underestimated by the balmer decrement (Hunt et al. 2001). This is certainly the case for NGC 5253-5 (Vanzì & Sauvage 2004) and He 2-10 (Cabanac et al. 2005).

The situation is more complex when considering the virial masses since they are affected by uncertainties that are difficult to quantify. In this case the discrepancies could be for different reasons. It could be that the HII regions are not virialized. A number of objections could indeed be raised to the virialization hypothesis, as the clusters are very young, and HII regions are typically irregular and short-living objects. In addition even under virialized conditions, the virial masses include both the stellar and the gas components. The gas-to-star ratio is unknown, but it can easily be on the order of 1 or more. The HII regions considered are larger than the stellar cluster; however, the total mass of the diffuse ISM is expected to be small. In the case of NGC 5253-5, for instance, half *FWHM* of the HII region spatial profile corresponds to 12.7 pc, while Calzetti et al. (1997) give a half light radius of the cluster of about 3 pc. Assuming a standard density of  $100 \text{ cm}^{-3}$ , the total mass of the diffuse gas in the volume observed would not exceed  $2 \times 10^4 M_{\odot}$ . The factor  $\eta$  is also uncertain as seen before. If we assume  $\eta = 10$  and a gas-to-star ratio of 1, we derive 8.6, 4.0, and  $66 \times 10^6 M_{\odot}$ , respectively, for the HII regions around clusters NGC 5253-1, -5, and He 2-10. The main uncertainty at this point is related to the assumption on the gas-to-star ratio.

The range of masses calculated by Vanzì & Sauvage (2004) for NGC 5253-5, assuming a Salpeter IMF, goes from 0.8 to  $2.1 \times 10^6 M_{\odot}$  for a lower mass cutoff between 1 and  $0.1 M_{\odot}$ , respectively. In this sense our virial estimate is consistent with a standard IMF. The most realistic value calculated for the mass of the cluster is  $1.2 \times 10^6$ , obtained using a Scalo IMF, which is flatter in the low mass regime and which extends from 0.1 to  $100 M_{\odot}$ .

We find that the comparison of the  $H\alpha$  fluxes and their broadening can complement the analysis of the IR light to derive the mass of YMCs.

### 3.2. Reddening

We derived the extinction in the spatial direction along the slit by using the observed  $H\alpha/H\beta$  ratio and assuming an intrinsic ratio of 2.86 (corresponding to  $T_e = 10000 \text{ K}$  and  $n_e = 100 \text{ cm}^{-3}$ , Hummer & Storey 1987). The results are shown in Fig. 4 and are consistent with previous determinations. Allen et al. (1976)

obtained  $A_V = 2.3$  in He 2-10 but with a larger aperture. Gonzalez-Riestra et al. (1987) obtained  $A_V = 1.27$  in NGC 5253 with an aperture similar to ours. We note that, in the case of NGC 5253-5, the extinction shows a marked maximum in the proximity of the cluster’s center, identified with position “0” in the plots, but shifted respect to it by a fraction of arcsec. The extinction in the other two cases shows a spatial gradient. Both facts can be understood if the central cluster breaks the molecular cloud in one preferential direction, as it is very often observed in the galactic HII regions. At about  $2''$  to the north of NGC 5253-1, the extinction increases at about the same location of the emission line region mentioned in Sect. 3.1.

### 3.3. Ionization status of the interstellar medium

We examined the spatial distribution of the ratios  $[OIII]/H\beta$  and  $[NII]/H\alpha$  as diagnostics of the ionization status of the ISM (Fig. 5). The line ratios show different spatial behaviors in the three clusters. In He 2-10 they share a trend with a maximum close to the position of the cluster. In NGC 5253 the two ratios are anti-correlated: in NGC 5253-1  $[NII]/H\alpha$  is maximum at the position of the cluster, while in NGC 5253-5 it is  $[OIII]/H\beta$  that peaks on the cluster center. We also note that a situation similar to the one observed in NGC 5253-5 is also present in the region to the north of NGC 5253-1. These clusters have diameters slightly smaller than  $1''$  in the HST images, therefore they are marginally resolved by our observations. As a consequence, we are confident that the line-ratio trend observed in Fig. 5 are real even within the cluster region. The errors on the line ratios are mostly determined by the spectro-photometry and are on the order of 2%.

We used CLOUDY (Ferland et al. 1998) to model the ratios observed and, in particular, to derive the effective temperature of the ionizing sources. The ionizing stellar spectra were approximated with black bodies. We used densities in the range  $10\text{--}100 \text{ cm}^{-3}$  (although the density does not affect significantly these ratios), and adopted the abundances known for the two galaxies: solar for He 2-10 and  $1/5 Z_{\odot}$  for NGC 5253. We varied the effective temperature of the ionizing stars  $T_*$  and the ionization parameter  $U$  to match the observed ratios. The use of both  $[OIII]/H\beta$  and  $[NII]/H\alpha$  allows us to remove the degeneracy between  $T_*$  and  $U$ . In Table 3 we compare the observed line ratios with the best fit obtained with CLOUDY, along with the inferred effective stellar temperatures  $T_*$  and the ionizing parameters  $U$ . These values are reported both for the position corresponding

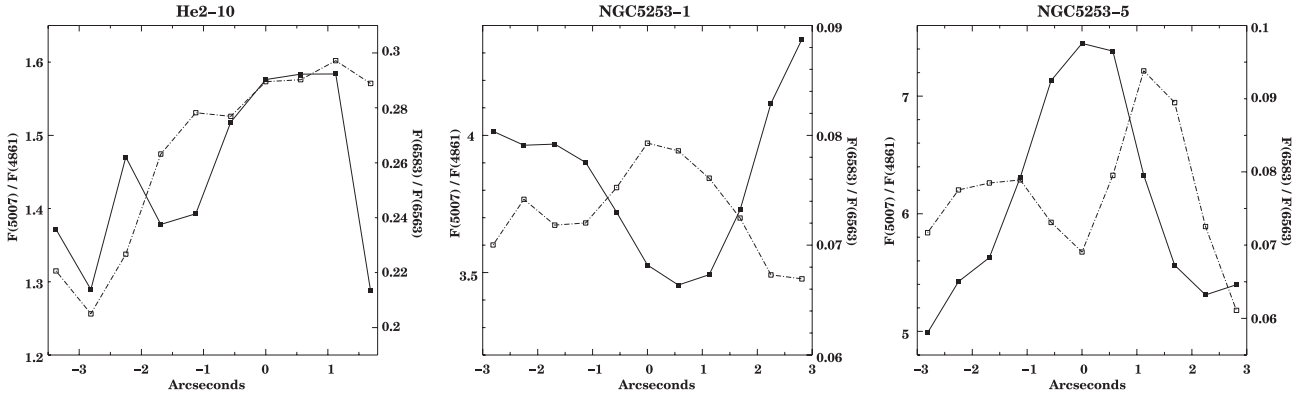


**Fig. 5.** Ratios of [OIII]/H $\beta$  (solid squares) for the three clusters. The vertical scale is on the lefthand axis and ratios of [NII]/H $\alpha$  (open squares) with the vertical scale displayed on the righthand axis.

**Table 3.** Line ratios observed (Cols. 2 and 3) and modeled with CLOUDY (Cols. 4 and 5) for the three clusters, on the cluster’s center (on) and at about 3’’ off center (off). The effective temperatures of the ionizing stars and the ionization parameter derived are given in the last two columns.

	[OIII]/H $\beta$ (ob)	[NII]/H $\alpha$ (ob)	[OIII]/H $\beta$	[NII]/H $\alpha$	$T_*$ (K)	Log $U$
5253-1 on	3.62	0.080	3.50	0.079	42 000	-1.7
5253-1 off	4.35	0.066	4.35	0.066	47 000	-2.1
5253-5 on	7.44	0.069	7.3	0.070	75 000	-2.0
5253-5 off	5.60	0.089	5.3	0.090	60 000	-2.1
He 2-10 on	1.57	0.29	1.62	0.30	62 000	-2.9
He 2-10 off	1.29	0.20	1.24	0.20	55 000	-2.7

to the cluster’s center (indicated as ON) and for the average of two locations (indicated as OFF), which lie at about 3’’ from the center. We find the two quantities well constrained by the observations; in particular, the uncertainties on  $T_*$  are about 2000 K. The observed ratios are corrected for the extinction.

The very high effective temperatures derived in the case of NGC 5253-5 and He 2-10 are not surprising as both are well-known WR galaxies (Schaerer et al. 1999). In both cases the presence of WR stars has been inferred by the HeII broad feature at 4686 Å. The WR stars are the evolved phase of the most massive stars, typically above 35  $M_{\odot}$  (Schaerer & Vacca 1998). They are very short-lived, less than 1 Myr (Maeder & Meynet 1994) and have effective temperatures above 30 000 K and up to  $10^5$  K (Maeder & Conti 1994). The cluster NGC 5253-1 instead shows lower  $T_*$ , consistent with its more advanced stage of evolution where the number of WR and O stars must be much reduced compared to the other two cases.

Even more interesting is the clear gradient in temperature observed in all cases across the clusters. Both He 2-10 and NGC 5253-5 have a higher temperature on the cluster’s center than in the outer parts, while NGC 5253-1 shows the opposite trend with higher temperature in the outer regions. NGC 5253-1 has an age of about 10 Myr, so the most massive stars of the cluster must have evolved already and produced the first supernovae; it is then plausible that the outer gas is ionized by other sources in the neighborhood of the cluster. In contrast the clusters observed in He 2-10 and NGC 5253-5 are both very young with ages of a few Myr, and indeed in these cases the hottest stars are observed in the central beam. Summarizing, in two cases we find indications of a higher density of massive stars toward the clusters’ centers. It is interesting to notice that the trend in the values of the line ratios is already observed in the apertures next to the central one, at 0.5’’ from the center, a distance that, at least in the case of NGC 5253-5, is comparable to the cluster’s size; see next section.

### 3.4. Mass segregation in YMCs?

Mass segregation has been previously observed in YMCs in the LMC (de Grijs et al. 2002a) and in M 82 (McCraday et al. 2005). In these cases the most massive stars appeared to be located toward the center of the cluster. An important question within this context is whether mass segregation in clusters is produced by dynamical effects or if it has instead a “primordial” origin, associated with the formation of the cluster itself. A way to answer this question is to compare the relaxation time with the age of the cluster (de Grijs et al. 2002b).

According to Vanzi & Sauvage (2004), NGC 5253-5 is possibly the youngest YMC observed, with an age <2 Myr. The relaxation time for this cluster can be derived using expression 6 of Meylan (1987). We measured the cluster radius on the optical HST images and obtained a  $FWHM$  of 0.45’’ in the  $F814W$  filter, or about 7 pc. We used a mass of  $1.2 \times 10^6 M_{\odot}$ . With these parameters, the relaxation time for a 100  $M_{\odot}$  star would be about 50 Myr, much longer than the age of the cluster. The relaxation time is even longer for less massive stars. The indication for mass segregation in NGC 5253-5 would therefore suggest a “primordial” rather than dynamical effect. The case for a “primordial” segregation in NGC5253-5 is even stronger than in the cluster R136, in 30-Dor, where mass segregation is also observed but the age of 3–4 Myr seems to be long enough, compared to the relaxation time, for dynamical effects to be relevant (Brandl et al. 1996).

### 3.5. Spectro-astrometry

The quality of our data allows us to employ the spectro-astrometry technique to resolve structures in the sources observed, beyond the limits imposed by the seeing. The technique is not new and has been described in detail by Bailey (1998a,b, and references therein). It consists of fitting the spatial profile of the source along the slit and determining its “centroid” as a

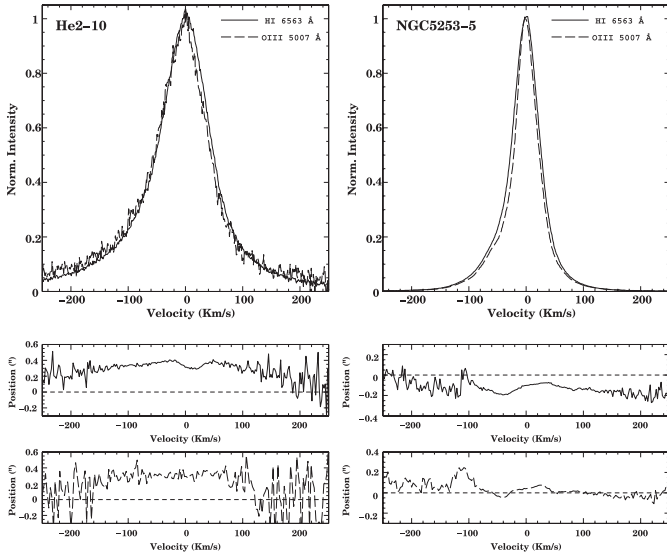


**Fig. 6.** Profiles of the  $H\alpha$  and [OIII] 5007 lines (*upper panel*). Position of the spatial centroid of  $H\alpha$  (*center pane*). Position of the spatial centroid of [OIII] (*bottom panel*). The position of the continuum is indicated by a dashed line in the center and bottom panels, while the 0 in the vertical scale indicate the average position of the emission line.

function of the wavelength, with a sub-pixel accuracy at the location of spectral features. If the source is extended or contains structures characterized by different spectral features, this will produce a displacement of the centroid of the composite spectrum along the slit. Due to the complexity of the regions observed, which typically include a bright compact source – the cluster – embedded into an extended and diffuse HII region, we have used two Gaussians to fit the spatial profile along the slit. Particular care was taken in the definition of the position of the continuum. Since the continuum signal is very faint in all cases, we summed up all the emission-line-free regions of the spectra in the direction of the dispersion and fit the spatial profile obtained in this way with a single Gaussian.

The results are shown in Fig. 6 for NGC 5253-5 and He 2-10. The quality of the data of NGC 5253-1 was not high enough to allow this kind of analysis. Both  $H\alpha$  and [OIII] 5007 lines have been used, the normalized line profiles are plotted in the upper panel of Fig. 6. It can be seen how the [OIII] line is in both cases slightly narrower than  $H\alpha$ . The displacements of the centroids as function of wavelength are shown in the middle and lower panels. The dashed lines indicate the position of the continuum corresponding to the 0 of the spatial scale. We observe that the emission lines tend to be shifted with respect to the continuum. The shift is about  $+0.20''$  for He 2-10 and  $-0.10''$  for the  $H\alpha$  in NGC 5253-5, equivalent to 8.7 and 1.6 pc, respectively. In other words, the stellar continuum and the gas emission do not come from the same region or, at least, their relative contribution is not uniform over the region observed. In NGC 5253-5, unlike  $H\alpha$ , the [OIII] profile is centered on the continuum. The origin of this difference is not clear; it could be physical (different [OIII] emitting regions relative to  $H\alpha$  or differential extinction between line and continuum emitting regions), but it could also be due to uncertainties in the determination of the continuum center, which is not well-constrained due to low signal-to-noise. We notice that an offset between the emission lines and the continuum has been observed, though on a larger scale, by Izotov et al. (1997) and Vanzì et al. (2000) in SBS 0335-052, so that it must be relatively common to giant HII regions. One possible explanation is

that the ISM surrounding the cluster be inhomogeneous and the molecular cloud be preferentially evaporated in one direction. In addition, the emission line centroid shows a structure at the position of the nominal center of the line, indicated with  $0 \text{ km s}^{-1}$ . In He 2-10 this structure is only detected in  $H\alpha$ , possibly because the [OIII] line does not have high enough signal-to-noise, while in NGC 5253-5 the same structure is detected in both lines. In both sources the size of this structure is about  $0.1''$  in size, corresponding to 1.6 and 4.3 pc, and it has a broadness  $70 \text{ km s}^{-1}$  and  $100 \text{ km s}^{-1}$  in velocity in He 2-10 and NGC 5253-5, respectively. These structures are difficult to interpret. Since they are relatively compact and are characterized by high velocities, they seem produced by local episodes of winds or by turbulence more than by the global structure of the regions observed. In fact, if we interpret these features as due to rotation, we can derive the mass from the size and velocity measured, simply as  $M = v^2 r / G$ . We obtained  $1.5 \times 10^6 M_\odot$  and  $4.3 \times 10^5 M_\odot$  for He 2-10 and NGC 5253-5, respectively.

## 4. Conclusions

We obtained high resolution spectra of three giant HII regions around YMCs hosted by blue dwarf galaxies. The main conclusions from the analysis of the data are the following.

1. The spectra are characterized by strong emission lines and a weak continuum. The line profiles can be fitted with two Gaussian components; in two cases one is broader than the other, with a typical width about four times larger.
2. We interpret the narrow component of the emission lines as being produced by a gas whose dynamics is mostly determined by gravity, and derive the associated virial masses.
3. The virial masses are highly uncertain; however, in all cases they exceed those obtained from the optical luminosities. In the case of NGC 5253-5, the virial mass and the mass obtained from the IR luminosity agree within a factor 2, suggesting the presence of a young stellar component hidden at optical wavelengths.
4. The observed mass of cluster NGC 5253-5 agrees with a standard IMF.
5. We attribute the broad component of the emission lines in the case of He 2-10 and NGC 5253-5 to turbulent gas or winds and detect inhomogeneities on the pc scale through the spectro-astrometry technique.
6. We observe indications of mass segregation in two clusters. In the case of NGC 5253-5 there is evidence for a primordial (i.e. intrinsic to the formation of the cluster), rather than dynamical origin of the segregation.

*Acknowledgements.* This research made use of the NASA/IPAC Extragalactic Database (NED), which is operated by the Jet Propulsion Laboratory, California Institute of Technology, under contract with the National Aeronautics and Space Administration. AS acknowledges the support of ESO under two studentships funded by the Director General Discretionary Funds. We thank the anonymous referee, who contributed very valuable comments that improved this paper, and Giovanni Cresci and Jorge Melnick for reading the manuscript and for useful discussions.

## References

- Allen, D. A., Wright, A. E., & Goss, W. M. 1976, MNRAS, 177, 91  
 Bailey, J. A. 1998a, Proc. SPIE, 3355, 932  
 Bailey, J. A. 1998b, MNRAS, 301, 161  
 Brandl, B., Sams B. J., Bertoldi, F., et al. 1996, ApJ, 466, 254  
 Cabanac, R., Vanzì L., & Sauvage, M. 2005, ApJ, 631, 252  
 Calzetti, D., Meurer, G. R., Bohlin, R. C., et al. 1997, AJ, 114, 1834

- Cresci, G., Vanzi L., & Sauvage M. 2005, A&A, 433, 447
- de Grijs, R., Johnson, R. A., Gilmore, G. F., & Frayn, C. M. 2002a, MNRAS, 331, 228
- de Grijs, R., Gilmore, G. F., Johnson, R. A., & Mackey, A. D. 2002b, MNRAS, 331, 245
- Fall, S. M., & Rees, M. J. 1977, MNRAS, 181, 37
- Fall, S. M., & Zhang, Q. 2001, ApJ 561, 751
- Ferland, G. J., Korista, K. T., Verner, D. A. et al. 1998, PASP 110, 761
- Fleck, J. J., Boily, C. M., Lançon, A., & Deiters, S. 2006, MNRAS, 369, 1392
- Galliano, E., Alloin, D., Pantin, E., Lagage, P. O., & Marco, O. 2005, A&A, 438, 803
- Gibson, B. K., Stetson, P. B., Freedman, W. L., et al. 2000, ApJ, 529, 723
- Gonzalez-Riestra, R., Rego, M., & Zamorano, J. 1987, A&A, 186, 64
- Hamuy, M., Walker A. R., Suntzeff, N. B., et al. 1992, PASP, 104, 533
- Hummer, D. G., & Storey, P. J. 1987, MNRAS, 224, 801
- Hunt, L. K., Vanzi, L., & Thuan, T. X. 2001, A&A, 377, 66
- Izotov, Y. I., Lipovetsky V. A., Chaffee, F. H., et al. 1997, ApJ, 476, 698
- Kobulnicky, H. A., Kennicutt, R. C., & Pizagno, J. L. 1999, ApJ, 514, 544
- Johansson, I. 1987, A&A, 182, 179
- Johnson, K. E., Leitherer C., Vacca W. D., & Conti, P. S. 2000, AJ, 120, 1273
- Larsen, S. S. 2000, MNRAS, 319, 893
- Larsen, S. S. 2002, AJ, 124, 1393
- Larsen, S. S., & Richtler, T. 1999, A&A, 345, 59
- Maeder, A., & Conti, P. S. 1994, ARA&A, 32, 227
- Maeder, A., & Meynet G. 1994, A&A, 287, 803
- McCrary, N., Graham, J. R., & Vacca, W. D. 2005, ApJ, 621, 278
- Melnick, J., Tenorio-Tagle, G., & Terlevich, R. 1999, MNRAS, 302, 677
- Meylan, G. 1987, A&A, 184, 144
- Rozas, M., Sabalisch, N., Beckman, J. E., & Knapen, J. H. 1998, A&A, 338, 15
- Schaerer, D., & Vacca, W. D. 1998, ApJ, 497, 618
- Schaerer, D., Contini T., & Pindao, M. 1999, A&AS, 136, 35
- Terlevich, R., & Melnick, J. 1981, MNRAS, 195, 839
- van den Bergh, S. 1980, PASP, 92, 122
- Vacca, W. D., Johnson, K. E., & Conti, P. S. 2002, AJ, 123, 772
- Vanzi, L., & Sauvage, M. 2004, A&A, 415, 509
- Vanzi, L., & Sauvage, M. 2005, A&A, 448, 471
- Vanzi, L., Hunt, L. K., Thuan, T. X., & Izotov, Y. I. 2000, A&A, 363, 493
- Whitmore, B. C., Zhang Q., Leitherer, et al. 1999, AJ, 118, 1551